Geophysical Research Letters

RESEARCH LETTER
10.1029/2018GL080602

Global Impacts of Arctic Sea Ice Loss Mediated by the Atlantic Meridional Overturning Circulation

Wei Liu[1] **and Alexey V. Fedorov**[2]

[1]Department of Earth Sciences, University of California, Riverside, CA, USA, [2]Department of Geology and Geophysics, Yale University, New Haven, CT, USA

Key Points:
- Global climate response to Arctic sea ice decline is markedly different on different timescales
- On shorter decadal timescales, Arctic sea ice decline causes a "bipolar seesaw" surface air temperature change and a northward ITCZ shift
- On multidecadal and longer timescales, Arctic sea ice decline leads to the weakening of the AMOC, mediating the direct impacts of sea ice

Supporting Information:
- Supporting Information S1

Correspondence to:
W. Liu,
wei.liu@ucr.edu

Citation:
Liu, W., & Fedorov, A. V. (2019). Global impacts of Arctic sea ice loss mediated by the Atlantic meridional overturning circulation. *Geophysical Research Letters*, *46*, 944–952. https://doi.org/10.1029/2018GL080602

Received 23 SEP 2018
Accepted 21 DEC 2018
Accepted article online 26 DEC 2018
Published online 29 JAN 2019

Abstract We explore the global impacts of Arctic sea ice decline in climate model perturbation experiments focusing on the temporal evolution of induced changes. We find that climate response to a realistic reduction in sea ice cover varies dramatically between shorter decadal and longer multidecadal to centennial timescales. During the first two decades, when atmospheric processes dominate, sea ice decline induces a "bipolar seesaw" pattern in surface temperature with warming in the Northern and cooling in the Southern Hemisphere, leading to a northward displacement of the Intertropical Convergence Zone and an expansion of Antarctic sea ice. In contrast, on multidecadal and longer timescales, the weakening of the Atlantic meridional overturning circulation, caused by upper-ocean buoyancy anomalies spreading from the Arctic, mediates direct sea ice impacts and nearly reverses the original response pattern outside the Arctic. The Southern Hemisphere warms, a Warming Hole emerges in the North Atlantic, the Intertropical Convergence Zone shifts southward, and Antarctic sea ice contracts.

Plain Language Summary To understand how the recent Arctic sea ice decline may affect global climate, we conduct model experiments in which we modify the properties of Arctic sea ice, in order to simulate an Arctic sea ice loss similar to the observed. We find that climate response shows dramatically different patterns during different periods after the imposed sea ice decline. During the first one or two decades, Arctic sea ice decline allows more solar energy into the Northern Hemisphere, altering the Earth's energy balance. As the Northern Hemisphere warms while the Southern Hemisphere cools, the tropical rain belt moves northward, and Antarctic sea ice expands. However, after several more decades to a century, the impacts from changes in the deep ocean become more important and eventually overwhelm the direct effects of sea ice loss on the atmosphere. The weakening of the Atlantic deep ocean circulation causes a cooling in the North Atlantic and a warming in the Southern Hemisphere. Antarctic sea ice contracts and the tropical rain belt shifts back to its original position and further south.

1. Introduction

According to satellite-derived data, Arctic sea ice has been declining over the past three to four decades (Ding et al., 2017; Parkinson & Cavalieri, 2008; Stroeve et al., 2007; also c.f., supporting information Figures S1 and S2a). This Arctic sea ice loss is now affecting the Earth's climate globally. In addition to changes in atmospheric circulation and wintertime weather in the northern midlatitude and high latitudes (e.g., Cohen et al., 2014; Francis et al., 2009; Overland & Wang, 2010; Screen et al., 2013, 2018), the effects of Arctic sea ice loss may extend to the tropics and the Southern Hemisphere (SH; e.g., Deser et al., 2015). One particular example is that variations in Arctic sea ice can modulate the latitudinal position of the Intertropical Convergence Zone (ITCZ; e.g., Chiang & Bitz, 2005). As shown in previous studies, in response to the reduction of Arctic sea ice cover, the ITCZ displaces northward in the absence of ocean dynamics (Cvijanovic et al., 2017; Cvijanovic & Chiang, 2013; Deser et al., 2015; Tomas et al., 2016) but can intensify equatorward when ocean dynamics are involved (Deser et al., 2015; Sun et al., 2018; Tomas et al., 2016). The equatorward ITCZ intensification may occur in the Pacific Ocean within ~25 years of ice loss due to enhanced warming in the eastern equatorial Pacific (K. Wang et al., 2018).

Moreover, Arctic sea ice decline can cause large-scale changes in ocean overturning circulation. Specifically, sea ice retreat generates positive buoyancy anomalies in the Arctic that can spread to the North Atlantic and induce the weakening of the Atlantic meridional overturning circulation (AMOC; e.g., Liu et al., 2019;

Oudar et al., 2017; Scinocca et al., 2009; Sévellec et al., 2017; Sun et al., 2018). In a different context, the impacts of weakened AMOC have been studied in freshwater hosing experiments, which show a robust southward shift of the ITCZ (e.g., Barreiro et al., 2008; Broccoli et al., 2006; Fedorov et al., 2007; Liu & Hu, 2015; Stouffer et al., 2006; Zhang & Delworth, 2005). Therefore, it is reasonable to anticipate that the sea-ice-induced AMOC change can play a critical role in mediating the more direct impacts of Arctic sea ice decline on the ITCZ shift. This interplay between atmospheric and oceanic processes driven by Arctic sea ice decline has not been explored in previous studies.

Accordingly, the goal of the present study is to explore global climate response to the reduction of Arctic sea ice cover and to study how it evolves in time, with a particular focus on the migration of the ITCZ and the role of the AMOC. To isolate the effects of Arctic sea ice loss from all other possible forcings, we apply an idealized perturbation approach in which we lower the albedo of Arctic sea ice in a fully coupled climate model (following Sévellec et al., 2017, and Liu et al., 2019). The decrease in albedo causes a rapid retreat of Arctic sea ice, which warms the Northern Hemisphere (NH) and initially induces a northward ITCZ displacement. However, we show that as the AMOC begins to slow down after the first two decades, the ITCZ shifts southward from its original position. This interplay between direct and indirect effects of Arctic sea ice decline on "fast" and "slow" timescales, overlooked in previous studies, should be critical for climate prediction on decadal to multidecadal and longer timescales.

2. Observations, Model Experiments, and the Energetics Framework

We use passive microwave sea ice concentration measurements from National Snow and Ice Data Center, which are based on gridded brightness temperatures from the Defense Meteorological Satellite Program series of passive microwave radiometers: the Special Sensor Microwave Imager and the Special Sensor Microwave Imager/Sounder. These sea ice concentration data have a resolution of 25 × 25 km. We use annual mean values of sea ice concentration (Figures S2a and S2b) and sea ice extent (Figure S1) that is defined as the area of ocean where ice concentration exceeds 15%.

For numerical simulations, we use Community Earth System Model (CESM), version 1.0.4, developed by the National Center for Atmospheric Research. The atmosphere (CAM4) and land components use a T31 spectral truncation. The ocean and sea ice components use an irregular horizontal grid with a nominal ~3° resolution that becomes significantly finer (~1°) close to Greenland and in the Arctic Ocean. Starting with a CESM preindustrial control run, we conduct ensemble perturbation experiments in which we lower the albedo of bare and ponded sea ice and snow cover on ice over the Arctic Ocean in the model sea ice component. Particularly, we change the standard deviation parameters of bare and ponded sea ice (R_{ice} and R_{pnd}) from 0 to −2 and reduce the single scattering albedo of snow by 10% for all spectral bands. This choice of parameters allows our perturbation experiments to closely replicate the observed Arctic sea ice loss during the past several decades, both in terms of spatial distribution (Figures S2a, S2c, and S2e) and the seasonal cycle change (Figure S3a). The perturbation experiments last 200 years.

Although this model simulates a larger sea ice area than the observed, which is typical for the lower-resolution configuration of CESM (Shields et al., 2012), the simulated wintertime deep convection (with the March mixed layer depth exceeding 400 m) occurs in the Norwegian Sea and extends to a region south of Iceland and east of the British Isles, that is, outside of the sea ice area (Figure S4). Therefore, sea ice retreat in the subpolar North Atlantic does not directly affect the deep convection sites.

To reduce the impact of model internal variability, we use an ensemble approach based on 10 ensemble members generated by slightly varying the initial condition of the model atmosphere component. We primarily present ensemble-mean results but include the ensemble spread in the figures for reference. Unlike previous studies (Deser et al., 2015; Sun et al., 2018; Tomas et al., 2016; K. Wang et al., 2018), our modified-albedo approach avoids using external heat flux anomalies to modulate the Arctic sea ice cover and thus ensures energy conservation in the climate system (Bitz et al., 2006; Blackport & Kushner, 2016, 2017; Cvijanovic et al., 2017; Graversen & Wang, 2009; Scinocca et al., 2009; Screen et al., 2018).

To evaluate Arctic sea ice changes in the perturbation experiments, we compute sea ice total area by integrating the ice fraction over the entire region of the ocean where ice forms. We use this metric because it is independent of the model grid and resolution (Eisenman et al., 2011) and can precisely describe the change

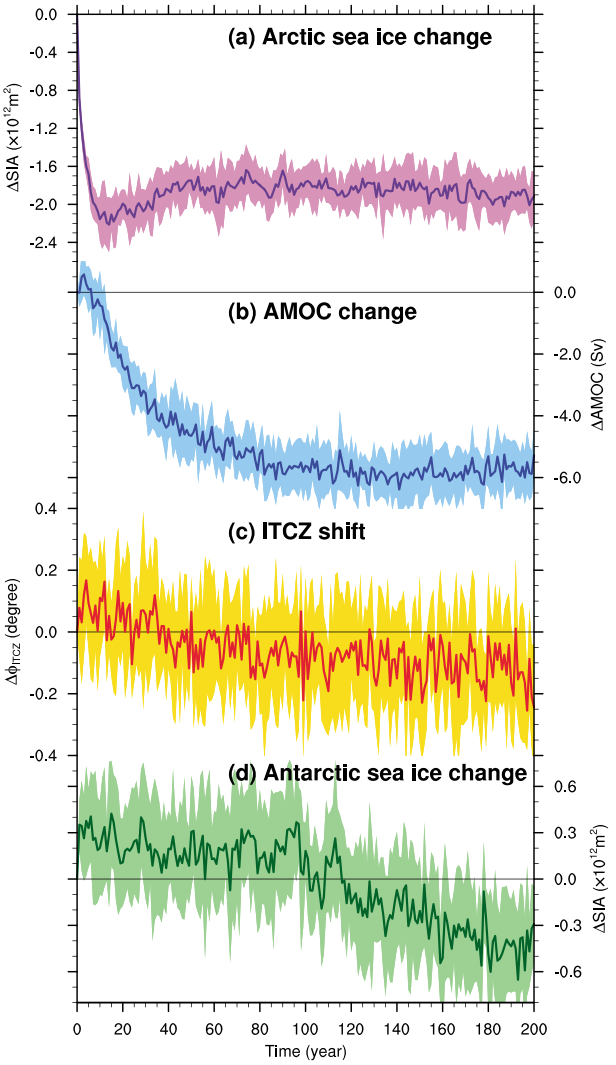

Figure 1. Changes in annual mean values for (a) Arctic sea ice total area, (b) AMOC strength, (c) global ITCZ latitudinal position, and (d) Antarctic sea ice total area in the perturbation experiments relative to a 50-year mean of the control run. Colored lines indicate ensemble means; color shading indicates ensemble spread estimated as one standard derivation from the ensemble mean. AMOC = Atlantic meridional overturning circulation; ITCZ = Intertropical Convergence Zone.

between sea ice and open water. The AMOC strength is defined as the maximum of annual mean meridional stream function below 500 m in the North Atlantic. The location of the ITCZ is estimated as the latitudinal centroid of precipitation:

$$\phi_{ITCZ} = \frac{\int_{\phi_1}^{\phi_2} \phi' \cos(\phi') P_r \mathrm{d}\phi'}{\int_{\phi_1}^{\phi_2} \cos(\phi') P_r \mathrm{d}\phi'}, \quad (1)$$

where $\phi_1 = 20^oS$ and $\phi_2 = 20^oN$ are the latitudinal bounds for integration and P_r denotes precipitation (Frierson & Hwang, 2012).

To access the roles of fast atmospheric processes due to the Arctic sea ice contraction versus the induced AMOC weakening, we adopt an energetics framework that links ITCZ displacement to energy fluxes into the atmosphere (e.g., Donohoe et al., 2013; Frierson & Hwang, 2012; Kang et al., 2008; Marshall et al., 2014; see T. Schneider et al., 2014 for a review). Since energy is transported primarily by the upper branch of the Hadley cell but water vapor by its lower branch, energy and water vapor are moved by the Hadley cell in opposite directions. Therefore, the ITCZ latitudinal position should shift in the opposite direction to changes in cross-equatorial atmospheric energy transport.

The atmospheric cross-equatorial energy transport ($\mathrm{AHT_{EQ}}$) can be calculated as

$$AHT_{EQ} = \frac{1}{2}[F_{ATM}(SH) - F_{ATM}(NH)], \quad (2)$$

where $F_{ATM}(SH)$ and $F_{ATM}(NH)$ are integrated energy fluxes entering the atmosphere in the SH and NH, respectively, and are calculated as

$$F_{ATM}(SH) = \int_{-\frac{\pi}{2}}^{0}\int_{0}^{2\pi} (F_{TOA} - F_{SFC}) a^2 \cos(\phi) \mathrm{d}\lambda \mathrm{d}\phi, \quad (3)$$

and

$$F_{ATM}(NH) = \int_{0}^{\frac{\pi}{2}}\int_{0}^{2\pi} (F_{TOA} - F_{SFC}) a^2 \cos(\phi) \mathrm{d}\lambda \mathrm{d}\phi, \quad (4)$$

where ϕ, λ, and a denote latitude, longitude, and the Earth's radius. F_{TOA} and F_{SFC} are energy fluxes at the top of the atmosphere (TOA) and at the ocean/land surface. Based on equations (2)–(4), any perturbation in climate components (such as Arctic sea ice loss or AMOC weakening) that changes F_{TOA} or F_{SFC} can affect the cross-equatorial energy transport in the atmosphere and hence the ITCZ position.

3. Results

Arctic sea ice and the AMOC in the perturbation experiment show markedly different temporal changes. In particular, the change of Arctic sea ice is rapid (Figure 1a) and takes 5–10 years. The diminished snow/ice albedo causes a loss of annual mean Arctic sea ice total area of ~1.9×10^6 km^2 (~12% of the control) during the 200-year simulation, with most of this loss occurring within the first few years of the run. In contrast, the AMOC changes much slower and shows no weakening during the first decade when ocean circulation anomalies are still confined to the Arctic Ocean and the Barents Sea, away from the North Atlantic deep convection regions (Liu et al., 2019). Only after the first 15 years, the AMOC starts weakening, as warm and fresh buoyancy anomalies induced by sea ice decline spread to the North Atlantic and suppress deep convection and the formation of North Atlantic deep water as described in detail in Sévellec et al. (2017) and Liu et al. (2019). About a century after the Arctic sea ice contraction, the AMOC loses ~6 Sv (~34% of the control, 1 Sv = 10^6 m^3/s) before leveling off. The sharp difference between the fast adjustment timescale for Arctic sea

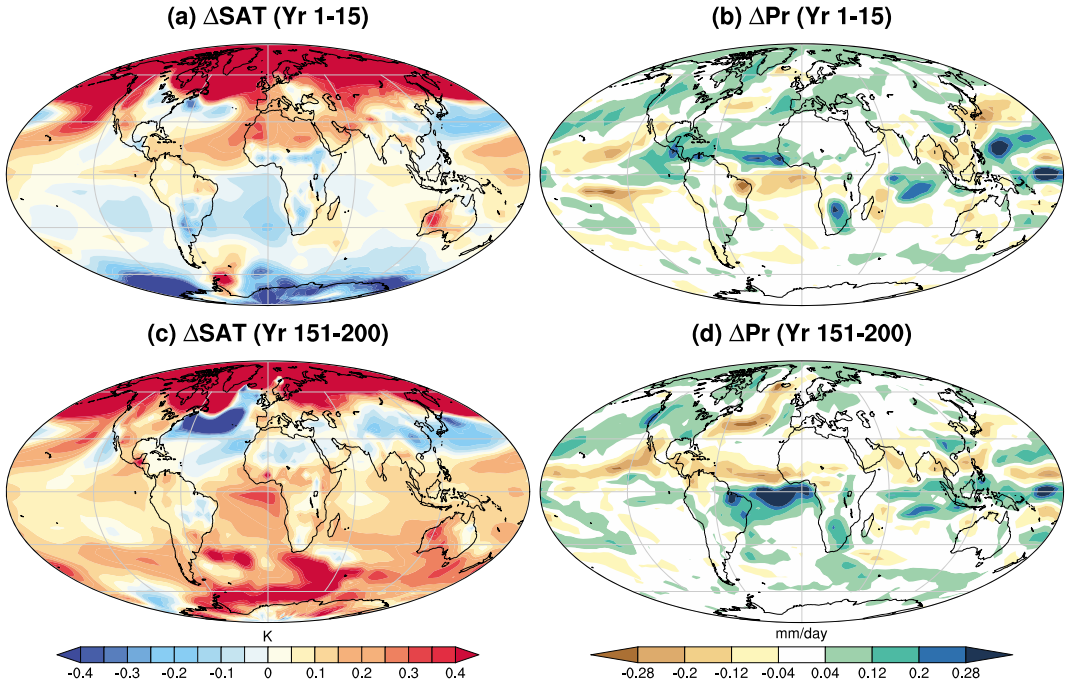

Figure 2. Anomalies in annual mean (a and c) surface air temperature (in K) and (b and d) precipitation (in mm/day) during (top) the first 15 years and (bottom) the last 50 years of the perturbation experiments. Anomalies are computed relative to a 50-year mean of the control run; ensemble-mean values are shown. Note the emergence of the North Atlantic Warming Hole and generally colder midlatitudes in (c) and the Atlantic ITCZ southward shift in (d).

ice and the slow timescale for the AMOC reflects the gradual adjustment of the North Atlantic Ocean to Arctic changes.

In response to Arctic sea ice and the subsequent AMOC changes, the ITCZ migration exhibits two distinct stages. The global ITCZ shifts northward by ~0.1° during the first 15 years (Figure 1c) of the Arctic sea ice rapid retreat (Figure 1a), whereas the AMOC remains largely unchanged, except for a small initial uptick (Figure 1b). As part of the ITCZ shift, rainfall increases north of the equator and decreases south of the equator over the tropical Atlantic and tropical eastern Pacific (Figure 2b). Anomalous surface air temperature shows a "bipolar seesaw": the Arctic and the rest of the NH warms, while the SH, including the Southern Ocean and parts of Antarctica, cools (Figures 2a and S5). The warming and cooling of the polar regions also extend to the lower and middle troposphere (Figure 4a). Following the changes in air temperature, the tropical rain belt shifts to the warmer hemisphere (i.e., to the NH). The rapid northward ITCZ shift is consistent with previous results obtained in slab-ocean climate models (Cvijanovic et al., 2017; Deser et al., 2015; Tomas et al., 2016; K. Wang et al., 2018) and a climate model with a full-depth ocean but fixed subsurface temperature and salinity (Smith et al., 2017), which confirms that the ITCZ northward shift is caused by atmospheric processes. Thus, the initial bipolar-seesaw temperature response is of atmospheric origin (Z. Wang et al., 2015) and is different from the typical signature of millennial variability related to AMOC changes often discussed in a paleoclimate context (e.g., Barker et al., 2009; Clark et al., 2002; Crowley, 1992; Rahmstorf, 2002).

The role of Arctic sea ice loss in the ITCZ shift can be further assessed via the energetics framework. Sea ice loss during the first 15 years induces a strong TOA radiation anomaly into the atmosphere over the Arctic (Figures 3a and S6a). This radiation anomaly is generated by enhanced shortwave radiation (Figure S6c) partially compensated by enhanced reflection from increased low clouds (Figures S6e and S7a) and is dampened by outgoing longwave radiation (Figure S6b). Outside the tropics (between 20°S and 20°N), the NH atmosphere on average gains 1.07 W/m^2 energy via the TOA, while a significant part of this energy gain (0.87 W/m^2) goes into the Arctic and midlatitude (30–60°N) Atlantic and Pacific Oceans in the form of ocean heat uptake (Figures 3b and S8a). Consequently, the NH atmosphere has a net energy gain owing to Arctic sea ice loss. In contrast, energy change in the extratropical SH atmosphere is much smaller (a loss

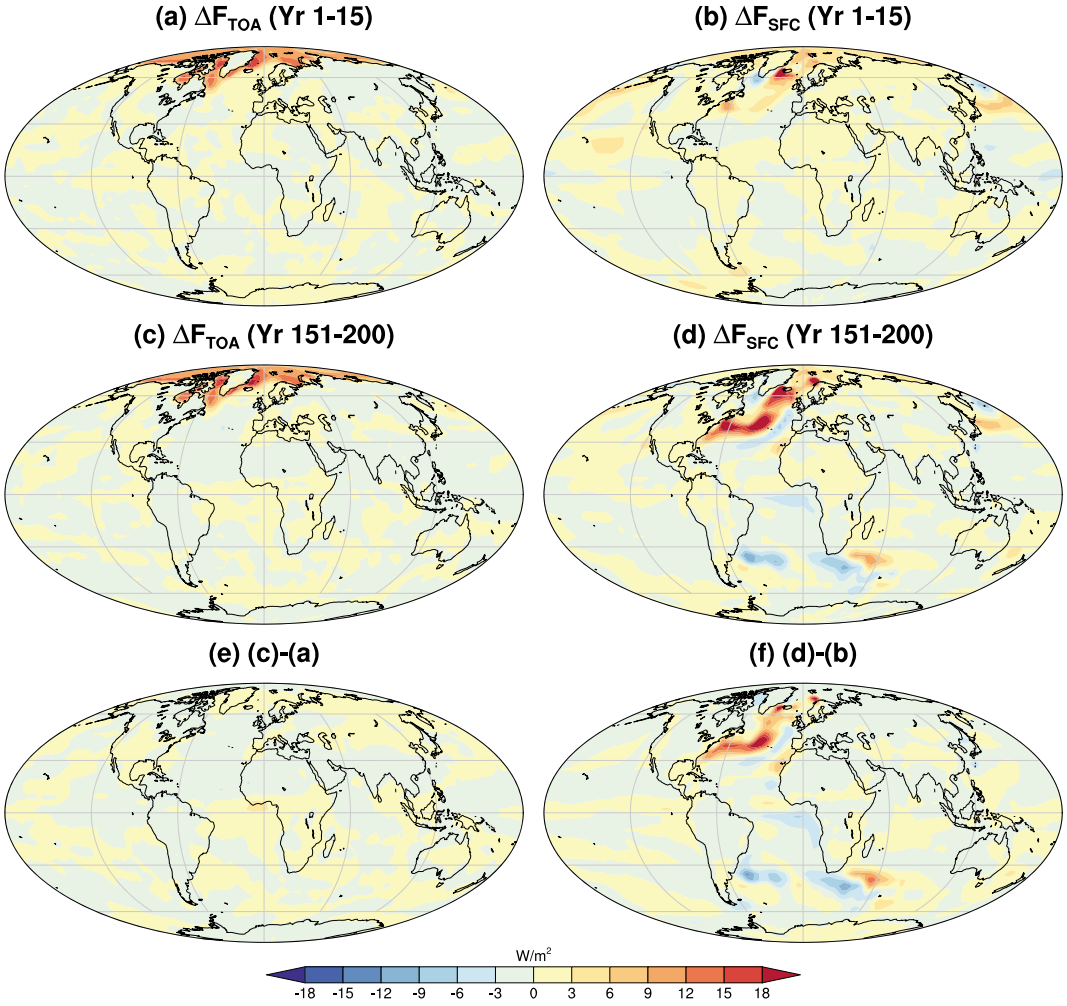

Figure 3. (a, c, and e) Changes in annual mean net energy flux at the top of atmosphere (in W/m^2, downward positive) during (a) the first 15 years and (c) the last 50 years of the perturbation experiments relative to a 50-year mean of the control run and (e) the difference between these two periods. (b, d, and f) As in the left panels but for changes in net energy flux at the ocean and land surfaces. Note the anomalous ocean heat uptake in the North Atlantic in (d).

of 0.07 W/m^2 via the TOA and a gain of 0.03 W/m^2 across the ocean/land surface). This interhemispheric energy imbalance thereby drives an anomalous southward cross-equatorial atmospheric energy transport ($AHT_{EQ} = -0.03$PW, 1PW = 10^{15}Watt; Figures S8a and S9), implying northward shifts of the Hadley cell (Figure S10a) and the ITCZ (Figure 1c).

After the first 15 years, the global ITCZ gradually begins shifting southward, moving to its original position after 40 years of the experiment and then shifting further ~0.12° (Figure 1c). The meridional ITCZ migration during this stage is associated with the slow response of the deep ocean or, more specifically, the weakening of the AMOC (Figure 1b). By the end of the experiment, rainfall decreases to the north of and increases to the south of the equator in the tropical Atlantic (Figure 2d), which is in line with the previous results from freshwater hosing experiments (e.g., Barreiro et al., 2008; Broccoli et al., 2006; Fedorov et al., 2007; Liu & Hu, 2015; Stouffer et al., 2006; Zhang & Delworth, 2005).

Surface air temperature shows a general warming over the globe except over the so-called "Warming Hole" in the North Atlantic (Figure 2c) and over northern midlatitudes, which results from the AMOC weakening. While Arctic sea ice loss is expected in general to induce global warming-like changes in surface air temperature at equilibrium (Deser et al., 2015; Sun et al., 2018; Tomas et al., 2016), the reduction in the AMOC and its heat transport causes a cooling of the North Atlantic and the atmosphere downstream of this region (e.g.,

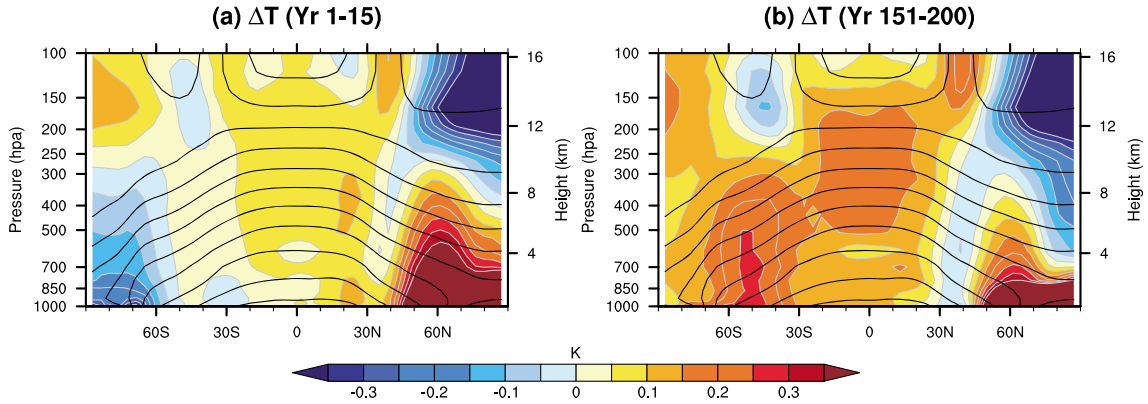

Figure 4. Changes in annual zonally-averaged air temperature (°C, colors) during (a) the first 15 years and (b) the last 50 years of the perturbation experiments relative to a 50-year mean of the control run. Contours indicate the climatological temperature (contour interval of 10 °C) in the control run.

Drijfhout et al., 2012; Liu et al., 2017; Rahmstorf et al., 2015; Sévellec et al., 2017). The Warming Hole enhances meridional temperature contrast in the tropical Atlantic, resulting in the Atlantic ITCZ shift toward the warmer hemisphere (i.e., the SH).

Above the surface, the longer-term response of air temperature shows a warming in the lower to middle troposphere at high latitudes and a pronounced upper tropospheric warming at low latitudes (Figure 4b), which is consistent with a "mini global warming" pattern invoked in Deser et al. (2015) and also present in other models (Blackport & Kushner, 2016, 2017; Screen et al., 2018).

Again, the AMOC effect on the ITCZ can be examined from the energetics perspective. Compared to the first 15 years, the TOA radiation anomaly associated with the Arctic sea ice loss has barely changed (Figures 3e and S8c) because the sea-ice-induced radiation adjustment via atmospheric processes was very rapid. However, large changes have occurred at the ocean surface—anomalous energy flux now goes into the ocean from the atmosphere in the North Atlantic over the Warming Hole region (Figures 3f and S8c). At the same time, energy flux into the ocean is reduced over the South Atlantic and the Atlantic sector of the Southern Ocean. These changes in ocean heat uptake (in the form of ocean surface heat fluxes) act as a negative feedback to the cooling in the North Atlantic and the warming in the South Atlantic and Southern Oceans (Figure S11; Armour et al., 2016).

Averaged over the extratropics, the NH atmosphere gains 0.97 W/m^2 of energy via the TOA during the last 50 years of the experiment (less by 0.10 W/m^2 than during the first 15 years) but loses 1.21 W/m^2 via the ocean surface (an increase of 0.34 W/m^2). In contrast to the first 15 years, the NH atmosphere now experiences a net energy loss due to the weakening of the AMOC. Meanwhile, the SH atmosphere loses 0.13 W/m^2 via the TOA and gains 0.35 W/m^2 via the ocean surface, so that it has a net energy gain. Thereby, the interhemispheric energy imbalance reverses relative to the first 15 years, driving an anomalous northward cross-equatorial atmospheric energy transport ($AHT_{EQ} = 0.12$PW; Figure S9), consistent with the southward shifts of the Hadley cell (Figure S10b) and the ITCZ (Figure 1c).

4. Conclusion and Implications

In this study, we have explored the mechanisms and timescales of global impacts of the contraction of Arctic sea ice cover. Specifically, we focus on the role of the interplay between faster atmospheric processes and a slower oceanic adjustment that involves the AMOC weakening. To investigate these fast and slow timescales, we conduct ensemble perturbation experiments with a fully coupled climate model wherein we reduce the albedo of snow/sea ice, causing a rapid contraction of Arctic sea ice cover comparable to the observed during the past three to four decades. We then monitor climatic changes during the first 200 years of the experiments. We find that climate response to Arctic sea ice decline is dramatically different on longer multidecadal to centennial timescales from that on shorter decadal timescales. Within one to two decades after the induced Arctic sea ice retreat, the global surface air temperature response

follows a bipolar seesaw pattern with a warmer NH and a colder SH. This fast response occurs mostly via atmospheric processes, as the ocean has little time to adjust to the forcing. As required by atmospheric energetics, the ITCZ shifts northward. In contrast, on longer multidecadal to centennial timescales, the ocean-mediated impacts become more important. As the AMOC weakens by 30–40%, the SH gradually warms and the ITCZ moves back, eventually shifting southward from its original position after ~40 years of the experiments. At the same time, while the Arctic remains warm, northern midlatitudes become slightly colder, with the largest cooling over the North Atlantic Warming Hole caused by the AMOC weakening.

This two-stage evolution of the ITCZ has important implications for global hydrological cycle. The fast ITCZ response to Arctic sea ice loss during the first stage is consistent with the northward ITCZ shift since the mid-1980s typically attributed to the reduction in atmospheric aerosols (Allen et al., 2015; H. Wang et al., 2016). Our results indicate that the Arctic sea ice retreat may have contributed to the northward displacement of the ITCZ, although the sea ice retreat itself may be partially caused by the aerosol reduction (Gagné et al., 2017; Navarro et al., 2016). It merits attention that in our study the perturbation to sea ice radiative balance is imposed instantaneously, and Arctic sea ice responds fairly quickly, within a few years. If a more gradual Arctic sea ice loss was imposed in the model (e.g., Sun et al., 2018), the ITCZ movement might be different. Also, precipitation response to Arctic sea ice loss differs between the current study and K. Wang et al. (2018), which can be due to the differences in the models used and/or sea ice perturbation methods.

Other implications of this study concern changes in Antarctic sea ice. At first, due to the cooling associated with the fast SH response to changes in the Arctic (Figure 2a), Antarctic sea ice grows (Figure 1d). In terms of total sea ice area, this sea ice growth is not unlike the observed Antarctic sea ice expansion during the satellite era (Figure S1), but there are differences in the magnitude, patterns, and seasonal changes (Figures S2 and S3b). The simulated Antarctic sea ice expansion occurs mainly over the Amundsen and the Ross Seas (Figure S2d) and is driven by atmospheric teleconnections. Specifically, Arctic sea ice loss brings about a reorganization of tropical convection (Figure S12c; Cvijanovic et al., 2017), which deepens the Amundsen Sea Low (Figure S12a) via an atmospheric Rossby wave train (Figure S12b). The deepened Amundsen Sea Low alters regional ocean circulation near Antarctica (D. P. Schneider & Deser, 2018), leading to Antarctic sea ice growth (Meehl et al., 2016). However, after about 100 years of the experiment, the SH warming (Figure S5) starts melting away Antarctic sea ice (Figure 1d), which primarily occurs east of the Antarctic Peninsula and around the East Antarctic (Figure S2f). The 100-year timescale is consistent with the period of AMOC weakening and is influenced by the slow ocean heat uptake in the Southern Ocean (Liu et al., 2018). Thus, our study yields new insights on the connection between climate change over the Arctic and the southern high latitudes.

Acknowledgments
This work was supported by grants from the DOE Office of Science (DE-SC0016538) and NSF (OCE-1756682 and OPP-1741841) and the Guggenheim Fellowship to A.V. F.; W. L. was also supported by the startup funds from the Department of Earth Sciences, University of California Riverside and the Regents Faculty Fellowship. Computations were performed at the Yale University Faculty of Arts and Sciences High Performance Computing Center. Sea ice observation data are publicly available at National Snow and Ice Data Center (https://nsidc.org/), and the Community Earth System Model is publicly available at http://www.cesm.ucar.edu/.

References

Allen, R. J., Evan, A. T., & Booth, B. B. B. (2015). Interhemispheric aerosol radiative forcing and tropical precipitation shifts during the late twentieth century. *Journal of Climate*, *28*, 8219–8246.

Armour, K. C., Marshall, J., Scott, J. R., Donohoe, A., & Newsom, E. R. (2016). Southern Ocean warming delayed by circumpolar upwelling and equatorward transport. *Nature Geoscience*, *9*, 549–554.

Barker, S., Diz, P., Vautravers, M. J., Pike, J., Knorr, G., Hall, I. R., & Broecker, W. S. (2009). Interhemispheric Atlantic seesaw response during the last deglaciation. *Nature*, *457*, 1097–1102.

Barreiro, M., Fedorov, A., Pacanowski, R., & Philander, S. G. (2008). Abrupt climate changes: How freshening of the northern Atlantic affects the thermohaline and wind-driven oceanic circulations. *Annual Review of Earth and Planetary Sciences*, *36*, 33–58.

Bitz, C. M., Gent, P. R., Woodgate, R. A., Holland, M. M., & Lindsay, R. (2006). The influence of sea ice on ocean heat uptake in response to increasing CO_2. *Journal of Climate*, *19*, 2437–2450.

Blackport, R., & Kushner, P. J. (2016). The transient and equilibrium climate response to rapid summertime sea ice loss in CCSM4. *Journal of Climate*, *29*, 401–417.

Blackport, R., & Kushner, P. J. (2017). Isolating the atmospheric circulation response to Arctic sea ice loss in the coupled climate system. *Journal of Climate*, *30*, 2163–2185.

Broccoli, A. J., Dahl, K. A., & Stouffer, R. J. (2006). Response of the ITCZ to Northern Hemisphere cooling. *Geophysical Research Letters*, *33*, L01702. https://doi.org/10.1029/2005GL024546

Chiang, J. C. H., & Bitz, C. M. (2005). Influence of high latitude ice cover on the marine intertropical convergence zone. *Climate Dynamics*, *25*, 477–496.

Clark, P. U., Pisias, N. G., Stocker, T. F., & Weaver, A. J. (2002). The role of the thermohaline circulation in abrupt climate change. *Nature*, *415*, 863–869.

Cohen, J., Screen, J. A., Furtado, J. C., Barlow, M., Whittleston, D., Coumou, D., et al. (2014). Recent Arctic amplification and extreme mid-latitude weather. *Nature Geoscience*, *7*, 627–637.

Crowley, T. J. (1992). North Atlantic deep water cools the southern hemisphere. *Paleoceanography*, *7*, 489–497.
Cvijanovic, I., & Chiang, J. C. H. (2013). Global energy budget changes to high latitude North Atlantic cooling and the tropical ITCZ response. *Climate Dynamics*, *40*, 1435–1452.
Cvijanovic, I., Santer, B. D., Bonfils, C., Lucas, D. D., Chiang, J. C. H., & Zimmerman, S. (2017). Future loss of Arctic sea-ice cover could drive a substantial decrease in California's rainfall. *Nature Communications*, *8*, 1947. https://doi.org/10.1038/s41467-017-01907-4
Deser, C., Tomas, R. A., & Sun, L. (2015). The role of ocean–atmosphere coupling in the zonal-mean atmospheric response to Arctic sea ice loss. *Journal of Climate*, *28*, 2168–2186.
Ding, Q., Schweiger, A., L'Heureux, M., Battisti, D. S., Po-Chedley, S., Johnson, N. C., et al. (2017). Influence of high-latitude atmospheric circulation changes on summertime Arctic sea ice. *Nature Climate Change*, *7*, 289–295.
Donohoe, A., Marshall, J., Ferreira, D., & Mcgee, D. (2013). The relationship between ITCZ location and cross-equatorial atmospheric heat transport: From the seasonal cycle to the last glacial maximum. *Journal of Climate*, *26*, 3597–3618.
Drijfhout, S., van Oldenborgh, G. J., & Cimatoribus, A. (2012). Is a decline of AMOC causing the warming hole above the North Atlantic in observed and modeled warming patterns? *Journal of Climate*, *25*, 8373–8379.
Eisenman, I., Schneider, T., Battisti, D. S., & Bitz, C. M. (2011). Consistent changes in the sea ice seasonal cycle in response to global warming. *Journal of Climate*, *24*, 5325–5335.
Fedorov, A., Barreiro, M., Boccaletti, G., Pacanowski, R., & Philander, S. G. (2007). The freshening of surface waters in high latitudes: Effects on the thermohaline and wind-driven circulations. *Journal of Physical Oceanography*, *37*, 896–907.
Francis, J. A., Chan, W., Leathers, D. J., Miller, J. R., & Veron, D. E. (2009). Winter Northern Hemisphere weather patterns remember summer Arctic sea-ice extentrctic sea-ice extent. *Geophysical Research Letters*, *36*, L07503. https://doi.org/10.1029/2009GL037274
Frierson, D. M. W., & Hwang, Y.-T. (2012). Extratropical influence on ITCZ shifts in slab ocean simulations of global warming. *Journal of Climate*, *25*, 720–733.
Gagné, M.-È., Fyfe, J. C., Gillett, N. P., Polyakov, I. V., & Flato, G. M. (2017). Aerosol-driven increase in Arctic sea ice over the middle of the twentieth century. *Geophysical Research Letters*, *44*, 7338–7346. https://doi.org/10.1002/2016GL071941
Graversen, R. G., & Wang, M. (2009). Polar amplification in a coupled climate model with locked albedo. *Climate Dynamics*, *33*, 629–643.
Kang, S. M., Held, I. M., Frierson, D. M. W., & Zhao, M. (2008). The response of the ITCZ to extratropical thermal forcing: Idealized slab-ocean experiments with a GCM. *Journal of Climate*, *21*, 3521–3532.
Liu, W., Fedorov, A., & Sévellec, F. (2019). The mechanisms of the Atlantic meridional overturning circulation slowdown induced by Arctic sea ice decline. *Journal of Climate*. https://doi.org/10.1175/JCLI-D-18-0231.1
Liu, W., & Hu, A. (2015). The role of the PMOC in modulating the deglacial shift of the ITCZ. *Climate Dynamics*, *45*, 3019–3034.
Liu, W., Lu, J., Xie, S.-P., & Fedorov, A. V. (2018). Southern Ocean heat uptake, redistribution, and storage in a warming climate: The role of meridional overturning circulation. *Journal of Climate*, *31*, 4727–4743.
Liu, W., Xie, S.-P., Liu, Z., & Zhu, J. (2017). Overlooked possibility of a collapsed Atlantic meridional overturning circulation in warming climate. *Science Advances*, *3*, e1601666.
Marshall, J., Donohoe, A., Ferreira, D., & McGee, D. (2014). The ocean's role in setting the mean position of the Inter-Tropical Convergence Zone. *Climate Dynamics*, *42*, 1967–1979.
Meehl, G. A., Arblaster, J. M., Bitz, C. M., Chung, C. T. Y., & Teng, H. (2016). Antarctic sea-ice expansion between 2000 and 2014 driven by tropical pacific decadal climate variability. *Nature Geoscience*, *9*, 590–595.
Navarro, J. A., Varma, V., Riipinen, I., Seland, Ø., Kirkevåg, A., Struthers, H., et al. (2016). Amplification of Arctic warming by past air pollution reductions in Europe. *Nature Geoscience*, *9*, 277–281.
Oudar, T., Sanchez-Gomez, E., Chauvin, F., Cattiaux, J., Terray, L., & Cassou, C. (2017). Respective roles of direct GHG radiative forcing and induced Arctic sea ice loss on the northern hemisphere atmospheric circulation. *Climate Dynamics*, *49*, 3693–3713.
Overland, J. E., & Wang, M. (2010). Large-scale atmospheric circulation changes are associated with the recent loss of Arctic sea ice. *Tellus*, *62*, 1–9.
Parkinson, C. L., & Cavalieri, D. J. (2008). Arctic sea ice variability and trends, 1979–2006. *Journal of Geophysical Research*, *113*, C07003. https://doi.org/10.1029/2007JC004558
Rahmstorf, S. (2002). Ocean circulation and climate during the past 120,000 years. *Nature*, *419*, 207–214.
Rahmstorf, S., Box, J. E., Feulner, G., Mann, M. E., Robinson, A., Rutherford, S., & Schaffernicht, E. J. (2015). Exceptional twentieth-century slowdown in Atlantic Ocean overturning circulation. *Nature Climate Change*, *5*, 475–480.
Schneider, D. P., & Deser, C. (2018). Tropically driven and externally forced patterns of Antarctic sea ice change: Reconciling observed and modeled trends. *Climate Dynamics*, *50*, 4599–4618.
Schneider, T., Bischoff, T., & Haug, G. H. (2014). Migrations and dynamics of the intertropical convergence zone. *Nature*, *513*, 45–53.
Scinocca, J. F., Reader, M. C., Plummer, D. A., Sigmond, M., Kushner, P. J., Shepherd, T. G., & Ravishankara, A. R. (2009). Impact of sudden Arctic sea ice loss on stratospheric polar ozone recovery. *Geophysical Research Letters*, *36*, L24701. https://doi.org/10.1029/2009GL041239
Screen, J. A., Deser, C., Smith, D. M., Zhang, X., Blackport, R., Kushner, P. J., et al. (2018). Consistency and discrepancy in the atmospheric response to Arctic sea-ice loss across climate models. *Nature Geoscience*, *11*, 155–163.
Screen, J. A., Simmonds, I., Deser, C., & Tomas, R. (2013). The atmospheric response to three decades of observed Arctic sea ice loss. *Journal of Climate*, *26*, 1230–1248.
Sévellec, F., Fedorov, A. V., & Liu, W. (2017). Arctic sea-ice decline weakens the Atlantic meridional overturning circulation. *Nature Climate Change*, *7*, 604–610.
Shields, C. A., Bailey, D. A., Danabasoglu, G., Jochum, M., Kiehl, J. T., Levis, S., & Park, S. (2012). The low-resolution CCSM4. *Journal of Climate*, *25*, 3993–4014.
Smith, D. M., Dunstone, N. J., Scaife, A. A., Fiedler, E. K., Copsey, D., & Hardiman, S. C. (2017). Atmospheric response to Arctic and Antarctic sea ice: The importance of ocean–atmosphere coupling and the background state. *Journal of Climate*, *30*, 4547–4565.
Stouffer, R. J., Yin, J., Gregory, J. M., Dixon, K. W., Spelman, M. J., Hurlin, W., et al. (2006). Investigating the causes of the response of the thermohaline circulation to past and future climate changes. *Journal of Climate*, *19*, 1365–1387.
Stroeve, J., Holland, M. M., Meier, W., Scambos, T., & Serreze, M. (2007). Arctic sea ice decline: Faster than forecast. *Geophysical Research Letters*, *34*, L09501. https://doi.org/10.1029/2007GL029703
Sun, L., Alexander, M., & Deser, C. (2018). Evolution of the global coupled climate response to Arctic sea ice loss during 1990–2090 and its contribution to climate change. *Journal of Climate*, *31*, 7823–7843.
Tomas, R. A., Deser, C., & Sun, L. (2016). The role of ocean heat transport in the global climate response to projected Arctic sea ice loss. *Journal of Climate*, *29*, 6841–6859.

Wang, H., Xie, S.-P., Tokinaga, H., Liu, Q., & Kosaka, Y. (2016). Detecting cross-equatorial wind change as a fingerprint of climate response to anthropogenic aerosol forcing. *Geophysical Research Letters*, *43*, 3444–3450. https://doi.org/10.1002/2016GL068521

Wang, K., Deser, C., Sun, L., & Tomas, R. A. (2018). Fast response of the tropics to an abrupt loss of Arctic sea ice via ocean dynamics. *Geophysical Research Letters*, *45*, 4264–4272. https://doi.org/10.1029/2018GL077325

Wang, Z., Zhang, X., Guan, Z., Sun, B., Yang, X., & Liu, C. (2015). An atmospheric origin of the multi-decadal bipolar seesaw. *Scientific Reports*, *5*, 8909.

Zhang, R., & Delworth, T. L. (2005). Simulated tropical response to a substantial weakening of the Atlantic thermohaline circulation. *Journal of Climate*, *18*, 1853–1860.